Heliyon 10 (2024) e23847

Contents lists available at ScienceDirect

Heliyon

journal homepage: www.cell.com/heliyon

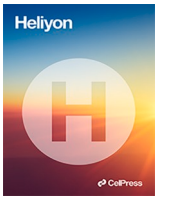

Mineral composition, crystallinity and dielectric evaluation of Bamboo Salt, Himalaya Salt, and Ba'kelalan salt content

Cheng Ee Meng [a,b,c,*], Che Wan Sharifah Robiah Mohamad [a], Nashrul Fazli Mohd Nasir [a,c], Khor Shing Fhan [d], Ong Hong Liang [a], Tan Xiao Jian [c,e,f], Lee Kim Yee [g], You Kok Yeow [h], Emma Ziezie Mohd Tarmizi [i], Mohd Riza Mohd Roslan [j], Siti Aishah Baharuddin [j]

[a] Faculty of Electronic Engineering & Technology, Universiti Malaysia Perlis (UniMAP), Arau, 02600, Malaysia
[b] Advanced Communication Engineering, Centre of Excellence (CoE), Universiti Malaysia Perlis (UniMAP), Kangar, 01000, Malaysia
[c] Sports Engineering Research Centre (SERC), Universiti Malaysia Perlis (UniMAP), Arau, 02600, Malaysia
[d] Faculty of Electrical Engineering & Technology, Universiti Malaysia Perlis (UniMAP), Arau, 02600, Malaysia
[e] Centre for Multimodal Signal Processing, Tunku Abdul Rahman University of Management and Technology (TAR UMT), Jalan Genting Kelang, Setapak, Kuala Lumpur, 53300, Malaysia
[f] Department of Electrical and Electronics Engineering, Faculty of Engineering and Technology, Tunku Abdul Rahman University of Management and Technology (TAR UMT), Jalan Genting Kelang, Setapak, Kuala Lumpur, 53300, Malaysia
[g] Lee Kong Chian Faculty of Engineering & Science, Sungai Long Campus, Tunku Abdul Rahman University, Jalan Sungai Long, Kajang, Cheras, Sungai Long City, 43000, Malaysia
[h] Department of Communication Engineering, Faculty of Electrical Engineering, Universiti Teknologi Malaysia, 81310, UTM Johor, Malaysia
[i] Centre of Foundation Studies for Agricultural Science, Universiti Putra Malaysia, Serdang, 43400, Malaysia
[j] Department of Engineering and Built Environment, Tunku Abdul Rahman University of Management and Technology, Penang Branch, Pulau Pinang, 11200, Malaysia

ARTICLE INFO

Keywords:
Mineral
Crystallinity
Dielectric
Salt
Composition

ABSTRACT

The mineral composition, crystallinity, and dielectric properties of salts can provide valuable insights into the quality and suitability of different types of salt for various applications. In this study, comprehensive analysis of the X-Ray Diffraction (XRD), X-ray fluorescence (XRF) and dielectric analysis of the Ba'kelalan salt, Himalaya salt and Bamboo salt have been investigated. The mineral composition of these salts, encompassing vital elements such as iodine and other trace minerals, significantly influences the salt's nutritional profile and overall excellence. Nonetheless, gauging the dispersion and density of these minerals poses difficulties due to conventional techniques that can be arduous, damaging, and expensive. Sample preparation is carried out before conducting X-ray diffraction (XRD), X-ray fluorescence (XRF), and dielectric analysis. XRD measurements are performed using the Bruker D2 Phaser to identify crystalline material phases. XRD operates on the principle of constructive X-ray interference within crystalline samples. For elemental analysis across a broad spectrum of materials, XRF is employed. Elemental peaks are scanned, starting from the lowest to the highest angle of incidence. The X-ray intensity at characteristic peaks is compared to the standard series. Dielectric spectroscopy analysis examines the dielectric behaviour of Ba'kelalan salt, Himalaya salt, and Bamboo salt. The setup involves a vector network analyser (VNA) paired with an open-ended coaxial probe, utilizing the microwave method. This approach ensures rapid, efficient, and non-destructive

* Corresponding author. Faculty of Electronic Engineering & Technology, Universiti Malaysia Perlis (UniMAP), Arau, 02600, Malaysia.
E-mail address: emcheng@unimap.edu.my (C.E. Meng).

https://doi.org/10.1016/j.heliyon.2023.e23847
Received 31 August 2023; Received in revised form 2 December 2023; Accepted 13 December 2023
Available online 17 December 2023

measurements of dielectric constants (ε′) and loss factors (ε”). The dielectric permittivity spectra are acquired within the frequency range of 4 GHz–20 GHz. ε′ of these salts increase with frequency. Meanwhile, ε” seem varies insignificantly over frequency. Mineral contents and crystallinity are the crucial factors lead to these responses. Based on the study, the quality and suitability of the selected salts for specific applications can be determined by considering their mineral composition, crystallinity, and dielectric properties in the context of the intended use. This gives an insight for some applications that may benefit from certain minerals or crystalline structures, others may require specific dielectric properties for effective use. Therefore, understanding these properties allows for decision-making in choosing the right type of salt for a given purpose, whether it's for foods, medical, industrial, healthcare, and technological applications.

1. Introduction

Minerals, classified as inorganic nutrients, are indispensable for maintaining specific physicochemical processes within the body's tissues [1]. The primary means of acquiring these minerals is by maintaining a well-rounded diet. Diverse minerals undertake distinct roles within the body, and their deficiency can lead to a range of illnesses. Conversely, an overabundance of minerals can disrupt homeostatic equilibrium and result in adverse toxic effects [1].

The origins of salt trace back to ancient times, intertwining with various facets of human history. Salt extraction methods encompassed diverse sources like sea water, saline lakes, brine springs, mineral deposits, and surface encrustations. In many inland regions, wood served as a fuel for brine evaporation, albeit this approach significantly contributed to widespread deforestation in central Europe [2]. Salt held a pivotal position in the economies of numerous areas, a fact often echoed in geographical names.

Salt stands as a vital mineral that harmonizes diverse physiological processes in both human bodies and other living organisms. Throughout history, salt has served as a valued preservative and essential flavour enhancer for countless generations [3]. From a chemical perspective, salt is an inherent combination of ionic compounds, primarily NaCl, finding widespread use in culinary and medicinal applications.

Naturally, salt exists as mineral halides containing sodium and chlorine elements. The mineral composition of salt differs depending on its origin, such as Bamboo salt, Himalaya salt, and Ba'kelalan salt. The excessive consumption of salt within a day can lead to hypernatremia [4], a condition characterized by a serum sodium concentration exceeding 145 mEq/L [5]. This can result in frequent vomiting and diarrhea, as the body aims to eliminate the excess salt.

Signs of salt toxicity emerge when sodium accumulates in the bloodstream, prompting the movement of water from cells into the blood to mitigate salt concentration. This elevation in blood volume impacts blood vessels and engenders extra strain on the heart. Over time, this strain can render blood vessels rigid, potentially culminating in conditions like stroke, heart attack, and hypertension. Furthermore, this fluid shift and subsequent brain fluid accumulation can induce coma, seizures, or even fatality. The accumulation of excess fluid in the lungs can impede breathing and potentially lead to heart failure. Notably, there is evidence that excessive salt intake may harm the heart, aorta, and kidneys without elevating blood pressure, while also potentially adversely affecting bone health. The ramifications of excessive salt consumption extend to various health risks and ailments, including chronic kidney disease, cardiovascular disorders, osteoporosis, and even cancer.

Salt has been an integral part of food preparation since ancient times, and its utilization remains customary in contemporary food manufacturing methods. While salt can be incorporated during cooking or added at the table, a substantial portion of dietary salt comes from processed foods [6]. Alongside sun or air dehydration and fermentation, salt constitutes a classical approach to food preservation, tracing back to prehistoric eras [7]. Historical techniques, such as immersing fish in saline solutions or soaking meat, facilitated extended preservation periods. Over time, this method was adapted to conserve a diverse array of foods [8].

Ba'kelalan salt originates from the mountains of northern Sarawak, where saltwater emerges from the ground. It is known for its delightful flavour and notable medicinal properties. Similarly, Bamboo salt hails from Korea, where sea salt is processed within bamboo trunks. This particular salt is renowned as a folk medicinal remedy for a range of ailments. It serves a significant role in the field of medicine, functioning as a gasotransmitter, exfoliator, anti-inflammatory agent, enhancer of antibiotic resistance, blood coagulator, and more. Himalayan salt, distinguished by its pink hue, is sourced from the Punjab region of Pakistan, near the foothills of the Himalayas. It contains no calories, protein, fat, carbohydrates, fibre, or sugar, yet it is abundant in sodium. Interestingly, these salts, along with common salt, can be employed for treating umbilical granuloma in neonates [9]. This treatment method is not only highly efficient but also cost-effective.

In various industries and scientific disciplines, selecting salts for specific applications presents a significant challenge, as it necessitates a comprehensive assessment of factors such as mineral composition, crystallinity, and dielectric properties. Limited research has focused on investigating salt through the dielectric approach for crystallinity and composition analysis, particularly in the case of Bamboo Salt, Himalaya Salt, and Ba'kelalan Salt. Extensive researches were conducted mainly on investigating dielectric properties of advanced materials, e.g. ceramics [10,11], magnetic materials [12,13], perovskite [14,15], and composites [16]. Therefore, this study endeavours to assess the potential of the dielectric method in determining the mineral composition of Bamboo Salt, Himalaya Salt, and Ba'kelalan Salt, with the support of crystallinity analysis. This knowledge gap results in suboptimal choices and impedes the realization of the full potential of salt-based solutions, particularly in the context of high-frequency dielectric properties. By offering a deeper understanding of the interplay between mineral composition, crystalline characteristics, and dielectric properties, this research contributes to enhance the efficiency and effectiveness of salt utilization across foods, medical, industrial, healthcare, and

technological domains.

2. Material and method

2.1. Crushing and grinding

Before subjecting the Himalaya salt, Bamboo salt, and Ba'kelalan salt to XRD, XRF, and dielectric measurements, they must first be pulverized into a powdered state [10]. Raw samples larger than 40 μm in size can result in undetected plane sets and insufficient crystallites, leading to imprecise intensity readings [17]. To facilitate subsequent grinding, each salt is initially crushed using a crusher to break down larger chunks. Following the crushing stage, the salts undergo grinding with a mortar and pestle. The crushed salt is then meticulously hand-ground using the same tools, yielding a fine powder. A well-ground sample measuring less than 40 μm in size should exhibit a lack of individual grain sensation when rubbed between fingers [18].

2.2. XRD

Utilizing the Bruker D2 Phaser XRD machine, the XRD measurements were conducted for the samples. XRD serves to discern the phase identification of crystalline materials, relying on constructive interference between monochromatic X-rays and the crystalline sample. Crystalline substances function as three-dimensional diffraction gratings for X-ray wavelengths, akin to the spacing of crystal lattice planes. The crystallinity phase of the salt samples was identified through XRD analysis, assessing the phase composition of the powdered samples.

In preparation for XRD measurement, the finely ground sample is positioned on a standard sample holder, typically featuring a plastic plate or disc housing a small cavity to accommodate the powdered material. Among mounting methods, top-loading is favoured for its ease of execution. To set up a top-loaded mount, the material is transferred into the sample holder, ensuring the cavity is entirely filled with the powder. Achieving the correct sample height and a smooth surface involves levelling off the cavity using a glass slide or razor blade. It's crucial not to compact or compress the powdered sample into the cavity, as this could result in non-random orientation of crystallites within the upper layer.

Examinations were performed within the range of 5°–90° 2θ, employing a step size of 0.1° and a scan rate of 2°/min. The analysis occurred using a powder diffractometer, utilizing Ni-filtered, Cu-Kα radiation ($\lambda = 1.54184$ Å). The filament current was set at 50 mA, while the accelerating voltage stood at 45 keV. Extraction of raw data was achieved through the application of HighScore Plus software [19].

2.3. XRF

The salt sample's elemental composition was ascertained using XRF. This method capitalizes on x-ray interaction with the material to unveil its elemental constituents. Employing a standard-less fundamental approach, Wavelength Dispersive X-ray Fluorescence (WDXRF) was utilized for quantitative elemental analysis of the salt samples. This technique incorporates the heightened fluorescent radiation stemming from secondary and tertiary excitation, thus reinforcing the credibility of the elemental analysis results for the salt samples.

The finely ground salt sample was loaded into a designated sample holder. Following this, the sample powder was compressed into pellets under a pelletizing pressure of 120 kN/cm^2 [20]. Subsequently, the sample holder was positioned within the vacuum chamber of the XRF ZSX Primus IV machine [21]. A 45° incidence and take-off angles were employed for scanning all samples using the X-ray tube. All measurements were performed thrice under vacuum conditions, incorporating activated sample rotation [20].

Fig. 1. The pellet form of (a) Himalaya salt (b) Ba'kelalan salt (c) Bamboo salt.

2.4. Pellet preparation

Prior to dielectric measurements, the Himalaya salt, Bamboo salt, and Ba'kelalan salt necessitate preparation in pellet form. The procedure begins by weighing 2g of the ground sample utilizing a digital electronic weighing scale. Subsequently, the sample is compacted into pellets through a hydraulic press. The powdered sample is introduced into a circular mold, which is then positioned at the hydraulic press's center. By engaging the lever, the required pressure is exerted onto the mold. This pressure, ranging from approximately 12 MPa–14 MPa, ensures the creation of a robust pellet from the 2g weighted salt sample. Fig. 1(a), (b) and (c) illustrates the resultant solid pellets, extracted from the circular molds, for Himalaya salt, Ba'kelalan salt and Bamboo salt, respectively.

2.5. Dielectric calibration

Two essential calibrations are requisite for both reflection and dielectric measurements. Calibration of reflection measurements is vital to account for potential phase errors that the dielectric probe could encounter during the measurement process. This calibration involves linking the coaxial cable to port 1 of the P-series Network Analyzer (PNA), with the other end connected to the calibration kit comprising "OPEN," "SHORT," and "LOAD" components, depicted in Fig. 2. To execute this calibration, initiate the 85052D software and navigate through the calibration wizard, sequentially performing the calibration steps for "OPEN," "SHORT," and "LOAD."

The calibration process for dielectric measurements commences by exposing the aperture of the high-temperature probe to the air, as depicted in Fig. 3(a). Subsequently, the conductor block is affixed to the high-temperature probe, as shown in Fig. 3(b). Ensuring a secure connection between the conductor block and the high-temperature probe is essential to prevent any presence of air voids. Following the calibration using the conductor block, the final calibration step entails utilizing 25 °C water as shown in Fig. 3(c). The flow of calibration step is as shown in Fig. 4. Throughout the dielectric measurement process, it's crucial for the aperture of the high-temperature probe to maintain contact with the pellet sample's surface, thus eliminating the potential for air voids.

2.6. pH and salinity

Before measuring pH and salinity, all samples are dissolved in distilled water. Each salt is weighed at 1.6667g using a digital electronic weighing scale. This weighed salt is then mixed with 50 ml of distilled water and stirred with a glass rod. Prior to measurement, calibration is conducted using the Multi-Parameter Pocket Water Quality Tester (pH and salinity multimeter). For pH meter calibration, buffer solutions with pH values of 4.0 (HI 7004), 7.0 (HI 7007), and 10.0 (HI 7010) are prepared, as depicted in Fig. 5(a). The pH meter's probe is immersed in the pH 7 buffer solution for 1–2 min, ensuring a reading of 7 for the measured pH value. This procedure is repeated with buffer solutions of pH 4 and pH 10.

Likewise, salinity testing necessitates calibration for precise results. The calibration procedure mirrors that of pH calibration. Small quantities of 35 ppt Salinity Calibration Solution are utilized, as illustrated in Fig. 5(b). The pH meter's probe is immersed in the 35 ppt salinity solution for 1–2 min, confirming the accurate reading as required.

2.7. Density

The density of a salt sample is a crucial physical property that provides essential insights into the relationship between its mass and volume. To measure the density, the first step involves accurately weighing the salt sample using a precise balance or scale. Following this, the volume occupied by the salt sample must be determined. In this work, density of Himalaya salt, Bamboo salt and Ba'kelalan salt is calculated using the Equation (1) [22].

$$p = \frac{m}{v} \tag{1}$$

The salt pellet is prepared with a mass and diameter of 2g and 2 cm, respectively.

Several factors can influence the density of a salt sample. Different types of salts have distinct densities, with variations arising from their chemical composition. Additionally, the crystalline structure, which determines the arrangement of salt molecules in a crystal

Fig. 2. Open, short and broadband load block of calibration kit.

Fig. 3. (a) Exposure aperture of the high temperature probe to the air. (b) Connect the high temperature probe to conductor block. (c) Contact the aperture of high temperature probe with the water.

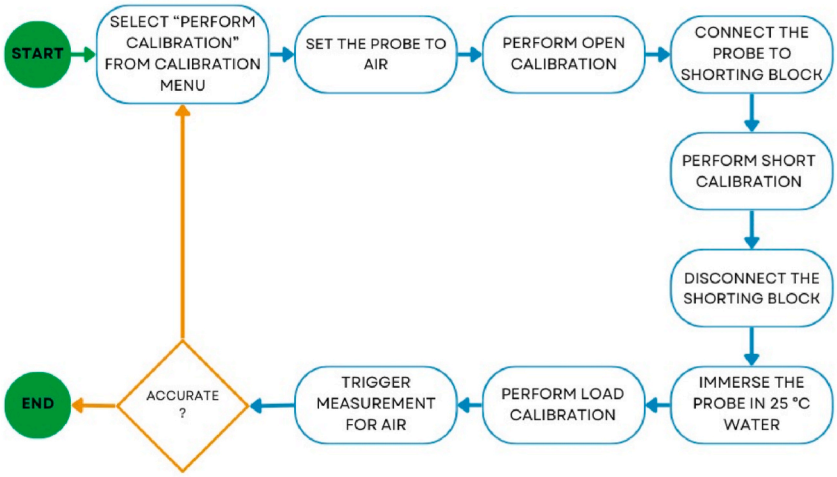

Fig. 4. Calibration of dielectric measurement using vector network analyzer.

Fig. 5. (a) Buffer solution with pH 4, pH 7 and pH 10. (b) 35 ppt Salinity solution.

lattice, can impact density. Alterations in temperature and pressure can also affect the density of a salt sample, with temperature increases typically leading to decreased density, while increased pressure tends to increase density.

3. Results and discussion

3.1. Relationship of XRD for Bamboo Salt, Himalaya Salt and Ba'kelalan salt

X-ray Diffraction (XRD) plays a pivotal role in salt sample measurements due to its multifaceted importance. Firstly, it enables the identification of crystal structures within salt samples, shedding light on how atoms or ions are arranged within their crystalline lattice. This information is fundamental for understanding the physical properties and behaviour of salts. XRD also excels in phase identification, especially in complex mixtures or when assessing impurities within salts, ensuring sample purity. In industrial contexts, XRD serves as a critical tool for quality control, verifying that salt products adhere to specific crystalline structure standards. Moreover, it empowers research and development efforts in areas such as materials science and chemistry, facilitating the exploration of salt properties and potential applications. XRD's utility extends to investigating phase transitions in salts, monitoring changes in crystal structure under varying conditions. Additionally, it aids in comprehending salt properties, stability, and reactivity. Finally, XRD finds application in environmental studies, particularly in the analysis of salt deposits and their ecological implications, making it an indispensable instrument for a wide spectrum of scientific, industrial, and quality assurance endeavours involving salt samples.

In this work, XRD measurements were conducted at room temperature within a diffraction angle range of 5°–90° (2θ). The step size was set at 0.1°, and the scan rate was maintained at 2°/min. Employing Ni-filtered, Cu-Kα radiation (λ = 1.54184 Å), a powder diffractometer was employed for sample analysis. The XRD spectra for Bamboo Salt, Himalaya Salt, and Ba'kelalan Salt are presented in Fig. 6.

The XRD spectral pattern depicted in Fig. 5 reveals distinct and noticeable peaks situated within the 2θ range of 31.4°–32.0° and 45.0°–45.8°. The highest peaks for each of the salts were pinpointed at 31.7° and 45.5°. Notably, the characteristic peaks derived from the analyzed salt samples closely align with the sodium chloride peaks documented in the JCPDS 78–0751 dataset at identical 2θ degrees. Confirmatory indexing of the diffraction patterns was carried out to validate the preliminary identification. Consequently, this outcome strongly suggests that all the samples exhibit a face-centred cubic structure [22], consistent with JCPDS card no. 78–0751 [23].

The XRD pattern findings for Himalaya salt are consistent with outcomes from previous investigations [24–26]. The examination unveiled XRD diffraction angles for Himalaya salt at 27.335°, 31.693°, 45.45°, 53.85°, 56.479°, 66.229°, 73.066°, 75.304°, and 83.973° [24]. Our Himalayan salt sample showcases a closely aligned angular pattern, featuring 27.35°, 31.70°, 45.43°, 53.86°, 56.46°, 66.21°, 73.02°, 75.25°, and 83.94°, as displayed in Table 1.

In summary, Ba'kelalan salt, Himalaya salt and Bamboo salt are commercially available. The XRD spectral patterns clearly exhibit distinct peaks falling within the 2θ range of 31.4°–32.0° and 45.0°–45.8°. The prominent peaks located at 31.7° and 45.5° for each salt align remarkably well with the sodium chloride peaks documented in the JCPDS 78–0751 dataset, corroborating their identification. This points to a consistent face-centred cubic crystal structure across all the analyzed samples, in line with JCPDS card no. 78–0751.

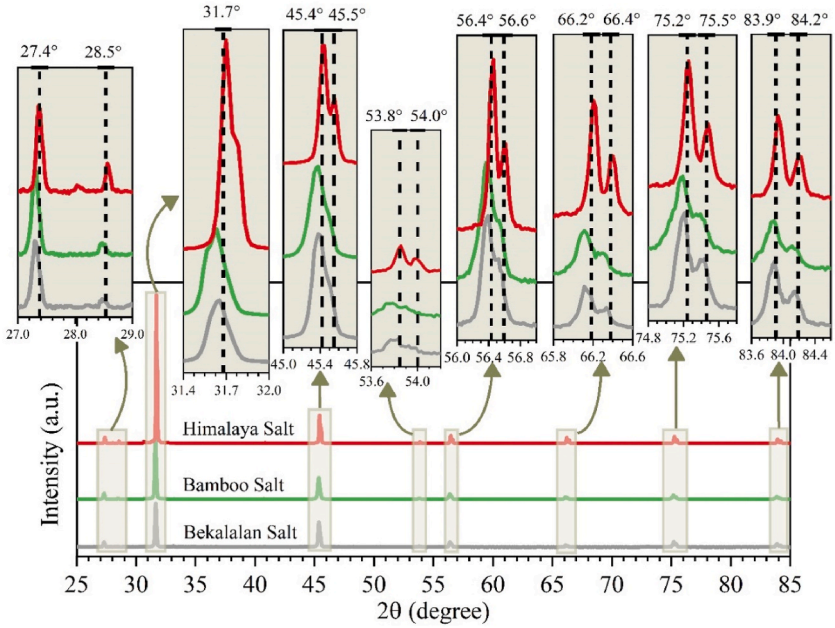

Fig. 6. XRD spectral patterns for Himalaya Salt, Bamboo Salt and Ba'kelalan Salt.

Table 1
The comparison of angular position of XRD of Himalaya salt, Bamboo salt and Ba'kelalan salt with data from *JCPDS 78–0751 for NaCl.

Salt	Peak 1	Peak 2	Peak 3	Peak 4	Peak 5	Peak 6	Peak 7	Peak 8	Peak 9
*NaCl	27.42°	31.76°	45.54°	53.98°	56.59°	66.37°	73.23°	75.46°	84.19°
Himalaya salt	27.35°	31.70°	45.43°	53.86°	56.46°	66.21°	73.02°	75.25°	83.94°
Bamboo salt	27.31°	31.63°	45.37°	53.78°	56.38°	66.11°	72.98°	75.18°	83.87°
Ba'kelalan salt	27.30°	31.65°	45.39°	53.79°	56.38°	66.12°	72.99°	75.20°	83.88°

3.2. Relationship of XRF for Bamboo Salt, Himalaya Salt and Ba'kelalan salt

On the other hand, X-ray Fluorescence (XRF) holds significant importance in salt sample measurements for its ability to analyse the elemental composition of salt samples swiftly and accurately. This analytical technique plays a pivotal role in quality control within industrial settings, ensuring salts meet specific elemental composition standards and maintain product consistency. XRF's exceptional sensitivity enables the detection of impurities or contaminants, even at trace levels, critical for assessing salt purity and safety, particularly in applications like food and pharmaceuticals. Moreover, it aids in nutritional profiling in the food industry, supporting research and development by providing insights into salt sample composition. Additionally, XRF finds utility in environmental studies, geological exploration, and the preservation of cultural heritage artifacts, making it an invaluable tool for diverse applications involving salt samples.

Fig. 7 presents the elemental composition analysis of Himalaya Salt, Bekalalan Salt, and Bamboo Salt through the X-Ray Fluorescence (XRF) Technique. Dominating the composition are two major elements, Na and Cl, with average concentrations of 35.38 ± 1.09 and 61.38 ± 0.56, respectively. All other elements detected were identified as minor and trace elements. Notably, the concentrations of Mg and S surpass 1 %, categorizing these elements as major constituents [20]. Himalaya salt and Bamboo salt exhibit elevated levels of the trace element magnesium, comprising 1.64 % and 2.01 %, respectively. Conversely, Ba'kelalan salt displays a notable trace element in the form of potassium, constituting 0.26 % of the total composition. Notably, Himalaya salt lacks the presence of Ni, while Ba'kelalan salt does not contain Zn. Bamboo salt, on the other hand, does not feature the presence of Ni and Zn.

Magnesium holds a crucial role in maintaining the normal structure of bones within the body. Its presence is essential for the proper growth and upkeep of bones, as well as for the optimal functioning of muscles, nerves, and various bodily systems. Additionally, magnesium aids in neutralizing stomach acid and facilitating the movement of stools through the intestine. While magnesium is acquired through dietary sources, instances of inadequate magnesium levels can arise. To address this, magnesium supplements become necessary. Notably, insufficient magnesium levels have been associated with conditions like stroke, diabetes, hereditary heart disease, arterial blockages, hypertension, and osteoporosis [27]. Based on dose-response data and human hazard evidence, the upper intake limit for magnesium is established at 350 mg [28].

Nickel, a vital micronutrient, plays a significant role in ensuring the effective functioning of the human body. It contributes to heightened hormonal activity and actively participates in lipid metabolism [29]. However, a cautious approach is necessary, as slightly exceeding daily intake by 1 mg can heighten the risk of undesirable side effects. Extended exposure to elevated levels of nickel or

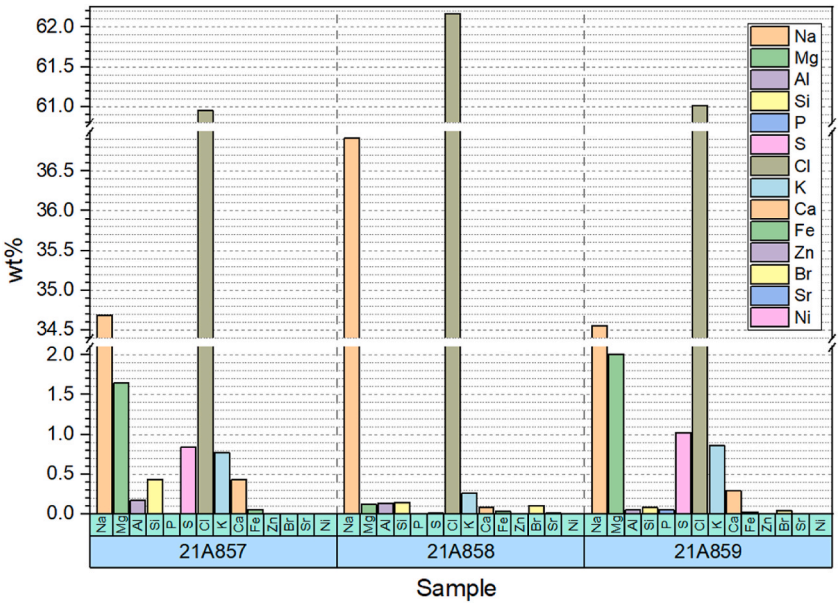

Fig. 7. XRF element composition.

excessive intake may lead to an array of adverse effects. The detrimental impacts of nickel encompass genotoxicity, haematotoxicity, teratogenicity, immunotoxicity, and the potential for carcinogenic effects [30].

Humans can absorb organic bromines through the skin, during breathing and with food. Organic bromines are widely used as sprays to kill insects and other unwanted pests. It also cause poisonous to larger animals such as human. Organic bromines can also cause damage to organs such as milt, lungs, kidneys and liver and they can cause stomach and gastrointestinal malfunctioning. Other forms of organic bromines, such as ethylene bromine, can even cause cancer. Humans absorb high doses of inorganic bromines through food and drinking water. These bromines can damage the thyroid gland and the nervous system [31]. According to the study, a recommended acceptable daily intake (ADI) of inorganic bromine for humans is one mg/kg body weight, based on a minimum pharmacologically effective dosage in humans of about 900 mg of potassium bromide, equivalent to 600 mg of bromide ion [29].

Bromine-based ingredients are used in treatment for many differing health problems and prescription drugs. Bromide ions have the ability to decrease the sensitivity of the central nervous system which makes them effective for use as anti-epileptics, tranquillizers and sedatives. This aids patients who suffer from seizures, or to babies who have colic, and is even used in expectorants, for cough medicine. Besides its use as a sedative, bromine-based medicine is also supplied to those suffering from hysteria, thyroid hyperactivity and heart problems [32].

In summary, the elemental composition analysis highlights the usage of the X-Ray Fluorescence (XRF) Technique to assess the composition of Himalaya Salt, Ba'kelalan Salt, and Bamboo Salt. Notably, sodium (Na) and chlorine (Cl) are the predominant elements, constituting the major portion of the composition. The analysis revealed other elements as minor and trace components, with magnesium (Mg) and sulphur (S) notably surpassing 1 % concentration, thus classified as major constituents. Additionally, variations in trace elements among the salts, such as elevated magnesium in Himalaya and Bamboo salt, and the presence of potassium in Ba'kelalan salt, accentuate the distinctive elemental profiles of these salts.

3.3. Relationship of dielectric constant (ε′) and loss factor (ε") with the frequency for bamboo salt, Himalaya salt and Ba'kelalan salt

The complex permittivity of a material, characterized by ε′ and ε'', plays a pivotal role in the analysis of its electrical behaviour at high frequencies. ε′ signifies the material's capacitive response, indicating its capacity to store electrical energy as an electric field. Conversely, ε'' denotes the material's dissipative behaviour, reflecting the extent to which it converts electrical energy into heat due to losses. Elevated ε′ values suggest excellent energy storage capacity, while elevated ε'' values indicate significant energy dissipation. The ratio ε''/ε′, known as the loss tangent (tan δ), quantifies the material's lossiness. In high-frequency applications, materials with low ε′ and ε'' are preferred to minimize energy loss and maximize signal transmission efficiency. This is vital for the design and optimization of performance in RF and microwave devices. The analysis of ε′ and ε'' at low frequencies, as depicted in Ref. [33], differ from the focus of this study. This study is centred on high-frequency applications (4 GHz–20 GHz), focusing on electromagnetic behavior in the radiofrequency and microwave spectrum. The dielectric characteristics of the salts were evaluated at high frequencies to distinguish their dielectric behaviors and uncover pertinent insights. A comprehensive frequency range spanning from 4 GHz to 20 GHz was employed to discern these properties. This frequency range is instrumental in facilitating a deeper understanding of the electrical properties of materials, quantifying salt concentrations in solutions, elucidating biological and medical processes, optimizing materials, scrutinizing electrochemical systems, monitoring environmental conditions, and evaluating food quality. Dielectric spectroscopy within this range yields valuable insights into the interactions between salts and other substances with electromagnetic fields across diverse frequencies, rendering it a versatile tool for both scientific and industrial applications. The dielectric attributes are delineated through the complex permittivity, expressed as $\varepsilon^* = \varepsilon' - j\,\varepsilon''$ [34,35]. Within the super high frequency (SHF) spectrum, the influence of polarization (including interfacial and dipolar polarization) accounts for the real component of complex permittivity (ε′), while energy dissipation effects (comprising conductivity and polarization losses) manifest as the imaginary component (ε") [34,36].

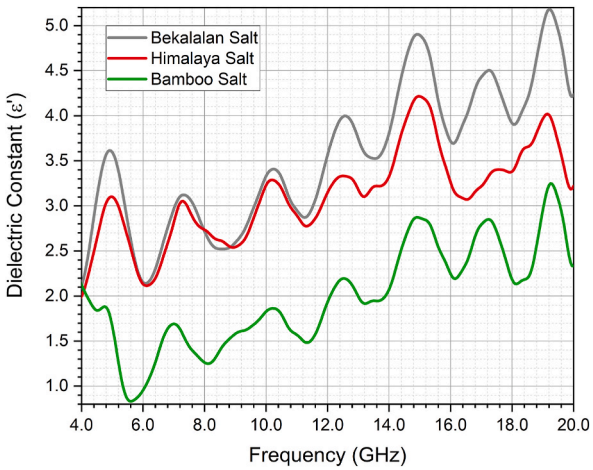

Fig. 8. ε′ of Bekalalan Salt, Himalaya Salt and Bamboo Salt against frequency (GHz).

Fig. 8 illustrates the variation of ε' (dielectric constant) for Ba'kelalan salt, Himalaya salt, and Bamboo salt across a frequency range of 4 GHz–20 GHz. Notably, each type of salt demonstrates its unique ε' profile as measured by the high-temperature dielectric probe. As frequency increases, ε' also exhibits an upward trend across all salts. This phenomenon arises from the interplay between the salt's crystal structures and the oscillating applied field, leading to significant effects on charge storage and dissipation. The intricate interactions within the crystal structures of these salts give rise to polarization and energy dissipation mechanisms, as well as their resultant frequency-dependent behaviors [34–37].

Ba'kelalan salt exhibits the highest ε' among the three salts in Fig. 8. This could be attributed to its notable effective absorption capacity and its pronounced polarization effects within the applied field. The frequency dispersion effect observed in different salts can be attributed to varying polarization mechanisms at play. These mechanisms contribute to the presentation of frequency-dispersive energy loss that differs based on the particular type of salt involved [38,39].

Fig. 9 illustrates the variation of ε" (dielectric loss factor) for Ba'kelalan salt, Himalaya salt, and Bamboo salt across the frequency range of 4 GHz–20 GHz. It is evident that different salts exhibit distinct values of dielectric loss factor as measured by the High-Temperature dielectric probe. As frequency increases, the dielectric loss factor for all salts demonstrates a decreasing trend. Notably, each relaxation step observed in the ε' spectrum depicted in Fig. 8 corresponds to a dielectric relaxation peak in the ε" spectrum, as shown in Fig. 9.

In both Figs. 8 and 9, it is observable that the ε' and ε" values of the permittivity spectrum exhibit fluctuations across frequencies, which underline the presence of various polarization mechanisms at play. These mechanisms contribute to the dynamic behavior of the material's permittivity properties.

For frequencies below 14 GHz, the ε' and ε" values demonstrate minimal variation. However, when the frequency surpasses 14 GHz, the dielectric loss factor (ε") for Bamboo salt and Himalaya salt becomes nearly identical, as depicted in Fig. 9. This phenomenon arises from the energy absorption attributed to the phase lag between dipole rotation and the applied field.

The propagation of electromagnetic waves within the crystal structure is significantly impacted by the salt's polarizability and the energy dissipation mechanisms within the crystal [34,37]. As a result, the salt displays distinct dielectric behavior, as presented in the permittivity spectra.

In general, the analysis of salt samples reveals a notable trend where increasing frequency corresponds to an increase in the dielectric constant. This phenomenon, known as frequency dispersion of the dielectric constant, can be attributed to several factors, including orientation polarization and interfacial polarization [40,41]. At lower frequencies, dielectric materials primarily respond to the applied electric field by aligning their electric dipoles. However, at higher frequencies (~kHz), the dipoles have insufficient time to respond to the rapidly changing electric field. Consequently, the effectiveness of orientation polarization diminishes at higher frequencies, resulting in an elevation of the dielectric constant [42]. Nevertheless, at higher frequencies (~GHz), the significance of interfaces between different phases or materials within a dielectric is pronounced. These interfaces contribute to interfacial polarization, thereby augmenting the dielectric constant [43]. The observed increase in the dielectric constant with frequency is a multifaceted phenomenon influenced by factors like electronic and interfacial polarization.

The loss factor and conductivity properties are crucial for understanding the electrical behaviour of materials and their wide-ranging applications [12,13,15,16]. The loss factor plays a vital role in dielectric material applications, affecting the efficiency and performance of electrical components and devices. Suresh et al. [10] have conducted an in-depth exploration of the significance of the loss factor in dielectric materials, providing comprehensive insights. Concurrently, understanding the frequency-dependent conductive behaviour is paramount in numerous scientific and industrial applications, ranging from capacitor design to impedance spectroscopy studies. Sivakumar et al. [11] have contributed valuable insights to this field, illuminating the topic of conductivity in dielectric materials, its frequency-dependent characteristics, and its relevance across scientific and industrial domains.

ε" describe energy dissipation or energy loss in material, the relation of conductivity (σ) and dielectric loss factor (ε") are shown in

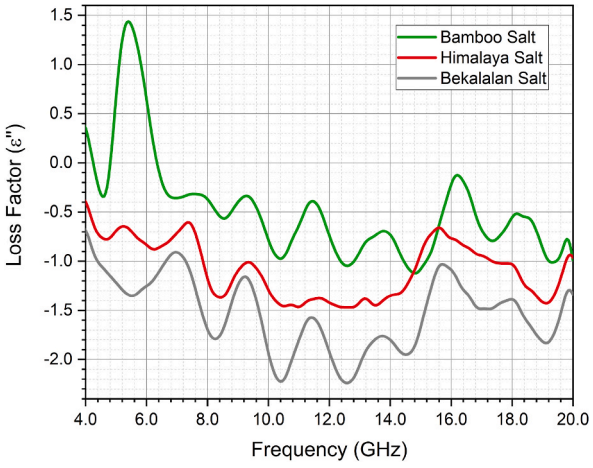

Fig. 9. ε" of Bekalalan Salt, Himalaya Salt and Bamboo Salt against Frequency (GHz).

Equation (2) [39].

$$\sigma = 2\pi f \varepsilon_0 \varepsilon'' \quad (2)$$

where the f is the frequency and ε_0 is the dielectric permittivity of vacuum. ε" is generally less than the ε' [44,45]. Referring to Equation (2), ε" is proportional to σ. Therefore, decreasing the ε" causes decrement of σ of material. Hence, ε′ decreases, because the capacity to store energy is decline due to increment of conduction loss.

Fig. 10 illustrates the trend of σ (conductivity) for Ba'kelalan salt, Himalaya salt, and Bamboo salt, showing a gradual decrease with increasing frequency. This behavior may stem from the characteristic ionic conductivity commonly seen in crystalline structures of ionic materials [46]. σ demonstrates minimal fluctuation at frequencies below 14 GHz. Interestingly, for frequencies beyond 14 GHz, the conductivity of Bamboo salt and Himalaya salt becomes indistinguishable, as depicted in Fig. 10. The rise in σ beyond 14 GHz can be attributed to the influence of space charge and cation disorder within their sites. As a result, σ at high frequencies displays frequency-dependent characteristics.

In the analysis of salt samples, an inverse trend has been identified, where an increase in frequency corresponds to a decrease in the loss factor. This reverse trend of a decreasing loss factor with increasing frequency in salt samples aligns with the behaviour observed in dielectric materials. It reflects the intricate interplay of polarization mechanisms, material properties, and measurement conditions. This understanding is valuable for assessing the electrical characteristics of salt samples in various applications. Similarly, a comparable trend has been observed in the analysis of salt samples, where increasing frequency leads to a decrease in conductivity. This reduction in conductivity with rising frequency can be ascribed to limited ion mobility and other contributing factors. At lower frequencies, ions have more time to move through the material, resulting in higher conductivity. Conversely, as frequency increases, ions have less time for migration, diminishing their mobility and impeding charge movement. Additionally, interfacial effects at material boundaries can hinder ion mobility, further contributing to the decline in conductivity at higher frequencies.

In summary, assessment of ε′ and ε" across a frequency range of 4 GHz–20 GHz was conducted on Ba'kelalan salt, Himalaya salt, and Bamboo salt. Notably, Ba'kelalan salt exhibited the highest ε′ due to its effective absorption capacity and pronounced polarization effects. The frequency-dependent variation in ε′ for all three salts, reflecting the intricate interactions within their crystal structures and the applied electromagnetic field. On the other hand, the distinctive values of ε" for different salts highlight their unique characteristics as measured by the High-Temperature dielectric probe. As frequency increases, ε" consistently decreases across salts, with relaxation peaks in ε′ corresponding to peaks in ε". The fluctuations in ε′ and ε" values across frequencies point to the diverse polarization mechanisms influencing material properties. Notably, for frequencies above 14 GHz, Bamboo salt and Himalaya salt exhibit similar ε" behaviour.

The conductivity (σ) trends of Ba'kelalan salt, Himalaya salt, and Bamboo salt, indicating a gradual decrease with increasing frequency. This behaviour is consistent with the ionic conductivity commonly observed in crystalline structures of ionic materials. The conductivity remains relatively stable at frequencies below 14 GHz, but beyond this threshold, the conductivity of Bamboo salt and Himalaya salt becomes similar due to the influence of space charge and cation disorder. This shift in conductivity at higher frequencies underscores the frequency-dependent nature of conductivity in these salts.

3.4. Relationship of density, pH and salinity for Bamboo Salt, Himalaya Salt and Ba'kelalan salt

Understanding the density of a salt sample is fundamental, offering valuable information applicable across various scientific, industrial, and practical contexts. Salt density plays a critical role in quality control across industries such as food, pharmaceuticals, and manufacturing, ensuring product consistency and quality. Furthermore, precise density data is invaluable in pharmaceuticals and

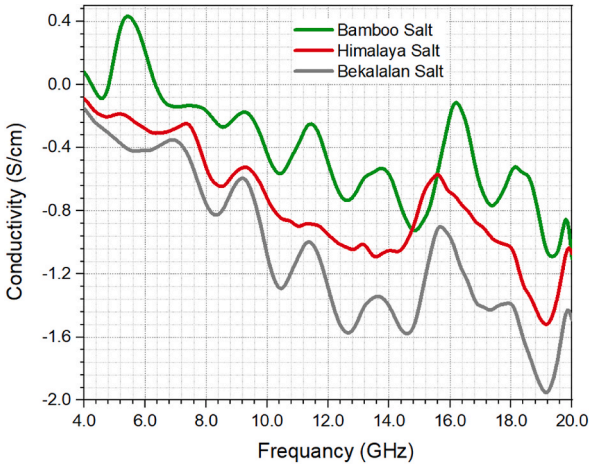

Fig. 10. The variation of conductivity (S/cm) of Ba'kelalan salt, Himalaya salt and Bamboo salt against frequency (GHz).

chemical manufacturing for dosing and formulation calculations. In environmental studies, density measurements of saltwater solutions are vital for understanding salinity levels and their effects on aquatic ecosystems. Additionally, researchers leverage density measurements to explore the physical properties and behaviour of salt-based materials in materials science, geology, and other scientific disciplines.

Conversely, a comprehensive understanding the pH of a salt sample is crucial for assessing its acidity or alkalinity in solution, influencing chemical reactions and suitability for various applications. Ramaprasad et al. [47], explores the impact of pH levels on the structural and magnetic properties of $CuFe_2O_4$ nanoparticles synthesized using a low-temperature hydrothermal technique. This study investigates how varying pH values influence the properties of these nanoparticles, shedding light on their potential applications in various fields. While Kumari et al. [48] provides valuable insights into the role of pH in shaping the properties of $BaTiO_3$ nanoparticles, which have significance in technological applications. pH measurement is fundamental in analytical methods, environmental studies, biological processes, and the food industry, making it a critical parameter in salt sample testing. Additionally, assessing the pH and salinity of a salt sample is essential for a comprehensive understanding of its chemical characteristics and suitability across different applications. These parameters hold significance in environmental, analytical, and industrial contexts, ensuring informed decision-making and proper control in relevant processes.

In Table 3, table salt act as a control in this study. pH value of table salt (NaCl) is within 6.7–7.3 [49]. The density of the table salt at the temperature of 25 °C is 2.17 g/cm^3 [50]. The density of the Himalaya salt is the highest, i.e. 2.20 ± 0.04 g/cm^3. This is probably due to mineral in Himalaya salt has higher atomic number cations which results in higher density [51].

Among the salts examined, Bamboo salt exhibits the highest pH value, as depicted in Table 3, with an average pH of 8.51 ± 0.03. It can be inferred that within concentrated brines, the dissociation of bicarbonate salts is suppressed, while it increases upon dilution, leading to the formation of hydroxide ions (OH^-) and subsequent pH elevation [52]. This underscores the influence of salinity on the pH value of salt [51]. Conversely, despite having the highest salinity level of 34.13 ± 0.30 ppt, table salt maintains a relatively low pH. This phenomenon can be attributed to the equilibrium between OH^- and H^+ ions within table salt.

The presence of additional elements in Bamboo salt, Himalaya salt, and Ba'kelalan salt leads to a scenario where the salt's anions can accept protons from water in a chemical reaction. This process results in the generation of OH^- ions. If the concentration of OH^- ions surpasses that of H^+ ions, an alkaline condition is established. Consequently, the pH values of Bamboo salt, Himalaya salt, and Ba'kelalan salt tend to exhibit a slightly alkaline nature.

The presence of Na+ and Cl-ions contributes to the elevation of salt's salinity level. Table salt, composed mainly of Na+ and Cl-ions, results in an increase in salinity. The XRF analysis presented in Table 2 indicates that Himalaya salt has comparatively lower levels of Na+ and Cl-ions contamination, specifically 34.681 % and 60.953 % respectively. Consequently, the salinity of Himalaya salt is lower in comparison to the other salts.

Among the salts, Himalaya salt possesses the highest density at 2.20 ± 0.04 g/cm^3. Notably, Bamboo salt stands out with the highest average pH of 8.51 ± 0.03, reflecting its increased hydroxide ion (OH-) formation upon dilution due to suppressed bicarbonate salt dissociation in concentrated brines, thereby influencing its pH value. Despite its higher salinity level, table salt maintains a lower pH due to the equilibrium between OH- and H+ ions within its composition.

4. Conclusion

In this study, X-ray Diffraction (XRD) spectral patterns reveal a consistent face-centred cubic crystal structure shared by all three salts, closely resembling the well-known sodium chloride (NaCl) structure. This observation plays a pivotal role in establishing their crystalline identity. Furthermore, an elemental composition analysis using X-ray Fluorescence (XRF) underscores the dominance of sodium (Na) and chlorine (Cl) in these salts. Additionally, minor and trace elements are present, with magnesium (Mg) and sulphur (S) emerging as notable major constituents. These distinctive elemental profiles emphasize the individuality of each salt. Moreover, dielectric analysis conducted over a frequency range of 4 GHz–20 GHz unveils unique dielectric behaviours. Ba'kelalan salt stands out with the highest dielectric constant (ε'), indicating effective absorption and polarization effects. This dielectric behaviour exhibits frequency-dependent variations influenced by mineral content and crystallinity. Conductivity trends indicate a gradual reduction in conductivity (σ) as the frequency increases, consistent with typical behaviour observed in ionic materials. Beyond 14 GHz, both Bamboo salt and Himalaya salt exhibit similar conductivity, hinting at the influence of space charge and cation disorder. On a different note, Himalaya salt boasts the highest density, measuring at 2.20 ± 0.04 g/cm^3, while Bamboo salt notably records the highest average pH level of 8.51 ± 0.03. These variations in pH and density can be attributed to differences in mineral composition and the formation of hydroxide ions (OH-). The implications of these findings are far-reaching and hold significant relevance across diverse applications. The mineral composition, crystallinity, and dielectric properties of these salts collectively impact their quality and suitability in culinary, industrial, scientific, and technological contexts. Specific applications may benefit from distinct minerals or crystalline structures, while dielectric properties influence effectiveness in scientific and technological applications. This comprehensive analysis equips decision-makers with valuable insights into the properties of Ba'kelalan salt, Himalaya salt, and Bamboo salt, facilitating informed choices for their utilization across a broad spectrum of fields.

Funding statement

The author is grateful to Universiti Malaysia Perlis, Perlis, Malaysia for the financial support granted to cover the publication fee of this research.

Table 2
XRF analysis of major element & trace element (WT%).

Element	Himalaya salt (21A857)	Ba'kelalan salt (21A858)	Bamboo salt (21A859)
Na	34.681	36.919	34.554
Mg	1.644	0.119	2.006
Al	0.175	0.132	0.052
Si	0.434	0.147	0.080
P	0.002	0.002	0.050
S	0.842	0.013	1.023
Cl	60.953	62.169	61.015
K	0.767	0.264	0.858
Ca	0.431	0.079	0.291
Fe	0.057	0.031	0.022
Zn	0.003	–	–
Ni	–	0.008	–
Br	0.008	0.108	0.041
Sr	0.003	0.011	0.007

Table 3
Density, pH and salinity of table salt, Bamboo salt, Himalaya salt and Ba'kelalan salt.

Salt	Density (g/ cm^3)	pH	Salinity (ppt)
Table salt (NaCl)	*2.17	6.21 ± 0.05	34.13 ± 0.30
Bekalalan salt	2.08 ± 0.04	8.27 ± 0.03	31.19 ± 0.29
Himalaya salt	2.20 ± 0.04	7.05 ± 0.25	30.14 ± 0.40
Bamboo salt	2.06 ± 0.01	8.51 ± 0.03	31.29 ± 0.39

Data availability statement

The data that has been used is confidential.

CRediT authorship contribution statement

Cheng Ee Meng: Writing - review & editing, Supervision, Methodology, Conceptualization. **Che Wan Sharifah Robiah Mohamad:** Methodology, Investigation. **Nashrul Fazli Mohd Nasir:** Conceptualization. **Khor Shing Fhan:** Methodology. **Ong Hong Liang:** Writing - original draft, Methodology. **Tan Xiao Jian:** Visualization, Validation, Formal analysis, Data curation. **Lee Kim Yee:** Writing - review & editing, Investigation, Formal analysis. **You Kok Yeow:** Software, Resources, Data curation. **Emma Ziezie Mohd Tarmizi:** Visualization, Software. **Mohd Riza Mohd Roslan:** Project administration, Formal analysis. **Siti Aishah Baharuddin:** Validation, Investigation.

Declaration of competing interest

The authors declare the following financial interests/personal relationships which may be considered as potential competing interests:CHENG EE MENG reports financial support and equipment, drugs, or supplies were provided by Maha Mangala Natural Health Products Pte. Ltd. If there are other authors, they declare that they have no known competing financial interests or personal relationships that could have appeared to influence the work reported in this paper.

Acknowledgments

The authors gratefully acknowledge Maha Mangala Natural Health Products Sdn. Bhd. for offering support in this project.

References

[1] M.A. Lee, Y.J. Choi, Y.S. Kim, S.Y. Chon, Y.B. Chun, S.H. Park, Y.R. Yun, et al., Effects of salt type on the metabolites and microbial community in kimchi fermentation, Heliyon 8 (2022), e11360.
[2] M. Cirillo, G. Capasso, V.A. Di Leo, N.G. De Santo, A history of salt, Am. J. Nephrol. 14 (1994) 426–431.
[3] S. Van Ruth, P. Dekker, E. Brouwer, M. Rozijn, S. Erasmus, D. Fitzpatrick, The sound of salts by broadband Acoustic Resonance Dissolution spectroscopy, Food Res. Int. 116 (2019) 1047–1058.
[4] H.J. Ju, H.J. Bae, D.E. Choi, K.R. Na, K.W. Lee, Y.T. Shin, Severe Hypernatremia by Excessive Bamboo Salt Ingestion in Healthy Young Woman, vol. 11, Electrolytes Blood Press, 2013, p. 53.
[5] Z.B. Wojszel, What serum Sodium concentration is suggestive for underhydration in geriatric patients? Nutrients 12 (2020) 496.
[6] E. Durack, M. Alonso-Gomez, M. Wilkinson, Salt: a review of its role in food science and public health, Curr. Nutr. Food Sci. 4 (2008) 290–297.
[7] W.G. Fahrenholtz, W. Fahrenholtz, Kinetics of composite formation by reactive metal penetration, J. Am. Ceram. Soc. 81 (2004) 2533–2541.
[8] I. Brandsma, Reducing sodium a European perspective, Food Technol. 60 (2006) 24–29.

[9] A.Z. Hossain, G.Z. Hasan, K.D. Islam, Therapeutic effect of common salt (table/cooking salt) on umbilical granuloma in infants, Bangladesh, J. Child Heal 34 (2012) 99–102.
[10] K.N. Suresh, R.P. Suvarna, K. Chandra Babu Naidu, Sol-gel synthesized and microwave heated $Pb_{0.8-y}La_yCo_{0.2}TiO_3$ (y= 0.2–0.8) nanoparticles: structural, morphological and dielectric properties, Ceram. Int. 44 (2018) 18189–18199.
[11] D. Sivakumar, K. Chandra Babu Naidu, K. Prem Nazeer, M. Mohamed Rafi, B. Sathyaseelan, G. Killivalavan, A. Ayisha Begam, Structural characterization and dielectric studies of superparamagnetic iron oxide nanoparticles, J. Korean Ceram. Soc. 55 (2018) 230–238.
[12] T. Vidya Sagar, T. Subba Rao, K. Chandra Babu Naidu, AC-electrical conductivity, magnetic susceptibility, dielectric modulus and impedance studies of sol-gel processed nano-NiMgZn ferrites, Mater. Chem. Phys. 258 (2021), 123902.
[13] A. Manohar, C. Krishnamoorthi, K. Chandra Babu Naidu, B. Palajonnala Narasaiah, Dielectric, magnetic Hyperthermia and Photocatalytic properties of $Mg_{0.7}Zn_{0.3}Fe_2O_4$ Nanocrystals, IEEE Trans. Magn. 56 (2020) 1–7.
[14] N. Suresh Kumar, R. Padma Suvarna, K. Rama Krishna Reddy, T. Anil Babu, S. Ramesh, B. Venkata Shiva Reddy, H. Manjunatha, et al., Tetragonal structure and dielectric behaviour of rare-earth substituted $La_{0.8}Co_{0.16-x}Eu_{0.04}Gd_xTiO_3$ (x= 0.04–0.16) nanorods, Mater. Chem. Phys. 278 (2022), 125598.
[15] P. Banerjee, N. Suresh Kumar, A. Franco Jr., A. Kumar Swain, K. Chandra Babu Naidu, X-band electromagnetic properties of hydrothermally synthesized $La_{1-x}Bi_xTiO_3$ (x= 0.2–0.8) nanoparticles, Inorg. Chem. Commun. 149 (2023), 110408.
[16] N. Suresh Kumar, R. Padma Suvarna, K. Chandra Babu Naidu, P.P. Mohapatra, P. Dobbidi, Insights into the dielectric loss mechanism of bianisotropic FeSi/SiC composite materials, ACS Omega 5 (2020) 25968–25972.
[17] J.V. Gilfrich, Book review: a practical guide for the preparation of specimens for X-ray fluorescence and X-ray diffraction analysis, X Ray Spectrom. 27 (1998) 349–350.
[18] R. Rudman, A practical guide for the preparation of specimens for X-ray fluorescence and X-ray diffraction analysis, J. Chem. Educ. 76 (1999) 762.
[19] I.A. Disher Al-Hydary, S.J. Edress Al-Mohana, M.M. Hussein Al-Marzooqee, Synthesis of highly crystalline phase pure calcium metastannate by molten salt method, Sci. Tech. Mater. 30 (2018) 103–108.
[20] A.A. Shaltout, S.I. Ahmed, S.D. Abayazeed, A. El-Taher, O.H. Abd-Elkader, Quantitative elemental analysis and natural radioactivity levels of mud and salt collected from the Dead Sea, Jordan, Microchem. J. 133 (2017) 352–357.
[21] M.M.A. Abdelhamid, B.G. Mousa, H. Waqas, M.A. Elkotb, S.M. Eldin, I. Munir, R. Ali, et al., Artificial thermal quenching and salt crystallization weathering processes for the assessment of long-term degradation characteristics of some sedimentary rocks, Egypt, Minerals 12 (2022) 1393.
[22] B. Zhang, Y. Wang, J. Yin, Y. Wang, H. Zhang, T. Csanádi, J. Dusza, et al., Carbon deficiency introduced plasticity of rock-salt-structured transition metal carbides, J. Mater. Sci. Technol. 164 (2023) 205–214.
[23] S.M. Abdou, H. Moharam, Characterization of table salt samples from different origins and ESR detection of the induced effects due to gamma irradiation, J. Phys. Conf. Ser 1253 (2019), 012036.
[24] V. Chander, D. Tewari, V. Negi, R. Singh, K. Upadhyaya, L. Aleya, Structural characterization of Himalayan black rock salt by SEM, XRD and in-vitro antioxidant activity, Sci. Total Environ. 748 (2020), 141269.
[25] K. AkashDilip, G.P. Krantikumar, Pharmaceutico-analytical evaluation of the bid lavana-aherbomineral formulation, Int. Ayurvedic Med. J. 1 (2017) 7.
[26] Ş. Yalçin, İ.H. Mutlu, Structural characterization of some table salt samples by XRD, ICP, FTIR and XRF Techniques, Acta Phys. Pol. A. 121 (2012) 50–52.
[27] A.M.A. Alawi, S.W. Majoni, H. Falhammar, Magnesium and human health: Perspectives and research Directions, Int J Endocrinol 2018 (2018), 9041694.
[28] H. Duggal, A. Bhalla, S. Kumar, J.S. Shahi, D. Mehta, Elemental analysis of condiments, food additives and edible salts using X-ray fluorescence technique, Int. J. Pharmaceut. Sci. Rev. Res. 35 (2015) 126–133.
[29] J. Yang, Z. Ma, Research progress on the effects of nickel on hormone secretion in the endocrine axis and on target organs, Ecotoxicol. Environ. Saf. 213 (2021), 112034.
[30] Z. Zdrojewicz, E. Popowicz, J. Winiarski, Nickel - role in human organism and toxic effects, Pol. Merkur. Lekarski 41 (2016) 115–118.
[31] S. Aggrey-Smith, Measurement of elemental compositions of selected tropical wood species – a case study of pra-anum forest, Ghana, Int. J. Biomed. Sci. Eng. 3 (2015) 34.
[32] R.C. Woody, MD, Bromide therapy for pediatric seizure disorder intractable to other antiepileptic drugs, J. Child Neurol. 5 (1990) 1.
[33] S.B. Aziz, O. Gh Abdullah, Rebar T. Abdulwahid, M.J. Ahmed, H.B. Tahir, S.R. Saeed, M.F.Z. Kadir, EDLC performance of plasticized NBG electrolyte inserted with $Ba(NO_3)_2$ salt: impedance, electrical and electrochemical properties, Electrochim. Acta 467 (2023), 143134.
[34] C.Y. Beh, E.M. Cheng, N.F. Mohd Nasir, S.K. Eng, M.S. Abdul Majid, M.J.M. Ridzuan, S.F. Khor, et al., Dielectric and material analysis on physicochemical activity of porous hydroxyapatite/cornstarch composites, Int. J. Biol. Macromol. 166 (2021) 1543–1553.
[35] X. Yin, L. Kong, L. Zhang, L. Cheng, N. Travitzky, P. Greil, Electromagnetic properties of Si–C–N based ceramics and composites, Int. Mater. Rev. 59 (2014) 326–355.
[36] S.J. Sondarva, D.V. Shah, Structural, complex dielectric, Ac conductivity and impedance properties of $Mn_{3-x}Cr_xTeO_6$ (x = 0.02, 0.04, 0.06 and 0.08) compounds, Solid State Sci. 134 (2022), 107043.
[37] M. Gałązka, N. Osiecka-Drewniak, Electric conductivity and electrode polarization as markers of phase transitions, Cryst 12 (2022) 1797.
[38] H. Weingartner, A. Knocks, Dielectric spectroscopy of the room temperature molten salt Ethylammonium Nitrate, J. Phys. Chem. A 105 (2001) 8646–8650.
[39] S. Hajra, M. Sahu, V. Purohit, R.N.P. Choudhary, Dielectric, conductivity and ferroelectric properties of lead-free electronic ceramic:$0.6Bi(Fe_{0.98}Ga_{0.02})O_3$-$0.4BaTiO_3$, Heliyon 5 (2019), e01654.
[40] K. Chandra Babu Naidu, Madhuri Wuppulluri, Ceramic nanoparticle synthesis at lower temperatures for LTCC and MMIC Technologies, IEEE Trans. Magn. 54 (2018), 2855663.
[41] K. Chandra Babu Naidu, Madhuri Wuppulluri, Microwave processed bulk and nano NiMg ferrites: a comparative study on X-band electromagnetic interference shielding properties, Mater. Chem. Phys. 187 (2017) 164–176.
[42] S. More, R. Dhokne, S. Moharil, Dielectric relaxation and electric modulus of polyvinyl alcohol–Zinc oxide composite films, Mater. Res. Express 4 (2017), 055302.
[43] S. Singha, M. Joy Thomas, Dielectric properties of epoxy nanocomposites, IEEE Trans. Dielectr. Electr. Insul. 15 (2008) 12–23.
[44] O. Amit, Y.K. Bentor, pH-dilution curves of saline waters, Chem. Geol. 7 (1971) 307–313.
[45] W.D. Williams, J.E. Sherwood, Definition and measurement of salinity in salt lakes, Int. J. Salt Lake Res. 3 (1994) 53–63.
[46] T. Zangina, J. Hassan, K.A. Matori, R.S. Azis, U. Ahmadu, A. See, Sintering behavior, ac conductivity and dielectric relaxation of $Li_{1.3}Ti_{1.7}Al_{0.3}(PO4)_3$ NASICON compound', Results Phys 6 (2016) 719–725.
[47] T. Ramaprasad, R. Jeevan Kumar, U. Naresh, M. Prakash, D. Kothandan, K. Chandra Babu Naidu, Effect of pH value on structural and magnetic properties of $CuFe_2O_4$ nanoparticles synthesized by low temperature hydrothermal technique, Mater. Res. Express 5 (2018), 095025.
[48] K. Pillalamarri Anita, D. Madhuri Devi, N. Satya Vijaya Kumar, Effect of pH on structure, Optical, and dielectric properties of $BaTiO_3$ nanoparticles, Cryst. Res. Technol. 58 (2023), 2300022.
[49] M.J. O'Neil, P.E. Heckelman, C.B. Koch, K.J. Roman, The Merck Index: an Encyclopedia of chemicals, drugs, and biologicals, J. Am. Chem. Soc. 129 (2007) 2197.
[50] J. Rissler, C. Preger, A.C. Eriksson, J.J. Lin, N.L. Prisle, B. Svenningsson, Missed evaporation from atmospherically relevant inorganic mixtures confounds experimental aerosol studies, Environ. Sci. Technol. 57 (2023) 2706–2714.
[51] S.A. Onaizi, Effect of salinity on the characteristics, pH-triggered demulsification and rheology of crude oil/water nanoemulsions, Sep. Purif. Technol. 281 (2022), 119956.
[52] M. Nasr, H.F. Zahran, Using of pH as a tool to predict salinity of groundwater for irrigation purpose using artificial neural network, Egypt, J. Aquat. Res. 40 (2014) 111–115.